

# Form factors and branching ratios of the FCNC $B \rightarrow a_1 \ell^+ \ell^-$ decays

R. Khosravi<sup>a</sup>

Department of Physics, Isfahan University of Technology, 84156-83111 Isfahan, Iran

Received: 10 June 2014 / Accepted: 9 May 2015 / Published online: 21 May 2015  
© The Author(s) 2015. This article is published with open access at Springerlink.com

**Abstract** We analyze the semileptonic  $B \rightarrow a_1 \ell^+ \ell^-$ ,  $\ell = \tau, \mu, e$  transitions in the framework of the three-point QCD sum rules in the standard model. These rare decays are governed by the flavor-changing neutral current transition of  $b \rightarrow d$ . Considering the quark condensate contributions, the relevant form factors as well as the branching fractions of these transitions are calculated.

## 1 Introduction

The decays governed by flavor-changing neutral current (FCNC) transitions are very sensitive to the gauge structure of the standard model (SM), which provides an excellent way to test such a model. These decays, prohibited at the tree level, take place at loop level by electroweak penguin and weak box diagrams. The FCNC transitions can be suppressed due to their proportionality to the small Cabibbo–Kobayashi–Maskawa matrix elements (for instance, see [1]). Among these, the FCNC semileptonic decays of the  $B$  meson occupy a special place in both experimental measurements and theoretical studies for the precision test of the SM due to the higher simplicity.

So far, the form factors of the semileptonic decay  $B \rightarrow a_1 \ell \nu$  have been studied via different approaches such as the covariant light front quark model (LFQM) [2], the constituent quark–meson model (CQM) [3], the light cone QCD sum rules (LCSR) [4], and the QCD sum rules (SR) [5]. However, the results obtained by these methods are different from each other.

In this work, we calculate the transition form factors of the FCNC semileptonic decays  $B \rightarrow a_1(1260) \ell^+ \ell^- / \nu \bar{\nu}$  in the framework of the three-point QCD sum rules method (3PSR). Considering the transition form factors for such decays in the framework of different theoretical methods has two-fold importance:

1. A number of the physical observables such as branching ratio, the forward–backward asymmetry and lepton polarization asymmetry, which have important roles in testing the SM and searching for new physics beyond the SM, could be investigated.
2. These form factors can also be used to determine the factorization of amplitudes in the non-leptonic two-body decays.

On the other hand, any experimental measurements of the present quantities and a comparison with the theoretical predictions can give valuable information as regards the FCNC transitions and strong interactions in  $B \rightarrow a_1 \ell^+ \ell^- / \nu \bar{\nu}$  decays.

The plan of the present paper is as follows: in Sect. 2, we describe the sum rules method to calculate the form factors of the FCNC  $B \rightarrow a_1$  transition. Section 3 is devoted to the numerical analysis of the form factors and branching ratio values of the semileptonic  $B \rightarrow a_1$  decays, with and without the long-distance (LD) effects.

## 2 Form factors of the FCNC $B \rightarrow a_1$ transition in 3PSR

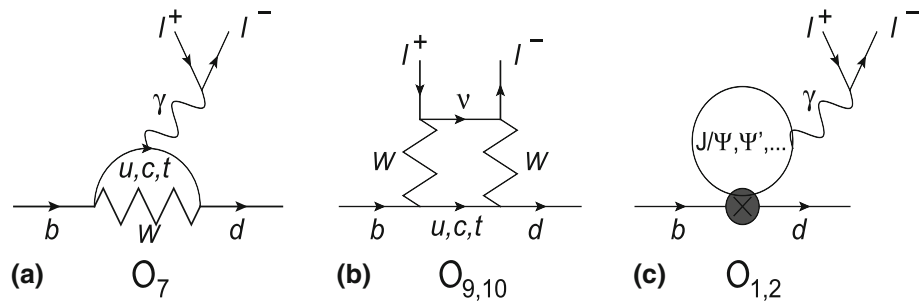
In the SM, the rare semileptonic decays which occur via  $b \rightarrow d \ell^+ \ell^-$  transition is described by the effective Hamiltonian [6]:

$$H_{\text{eff}} = -\frac{G_F}{\sqrt{2}} V_{tb} V_{td}^* \sum_{i=1}^{10} C_i(\mu) O_i(\mu), \quad (1)$$

where  $V_{tb}$  and  $V_{td}$  are the elements of the CKM matrix, and  $C_i(\mu)$  are the Wilson coefficients. It should be noted that the CKM-suppressed contributions proportional to  $V_{ub} V_{ud}^*$  are neglected, and also the approximation  $|V_{tb} V_{td}^*| \simeq |V_{cb} V_{cd}^*|$  is adopted [7]. The standard set of the local operators for the  $b \rightarrow d \ell^+ \ell^-$  transition is written as [8]

<sup>a</sup>e-mail: rezakhosravi@cc.iut.ac.ir

**Fig. 1** **a, b**  $O_7$  and  $O_{9,10}$  short-distance contributions. **c**  $O_{1,2}$  long-distance charm-loop contribution



$$\begin{aligned}
 O_1 &= (\bar{d}_i c_j)_{V-A}, (\bar{c}_j b_i)_{V-A}, \\
 O_2 &= (\bar{d}c)_{V-A} (\bar{c}b)_{V-A}, \\
 O_3 &= (\bar{d}b)_{V-A} \sum_q (\bar{q}q)_{V-A}, \\
 O_4 &= (\bar{d}_i b_j)_{V-A} \sum_q (\bar{q}_j q_i)_{V-A}, \\
 O_5 &= (\bar{d}b)_{V-A} \sum_q (\bar{q}q)_{V+A}, \\
 O_6 &= (\bar{d}_i b_j)_{V-A} \sum_q (\bar{q}_j q_i)_{V+A}, \\
 O_7 &= \frac{e}{8\pi^2} m_b (\bar{d} \sigma^{\mu\nu} (1 + \gamma_5) b) F_{\mu\nu}, \\
 O_8 &= \frac{g}{8\pi^2} m_b (\bar{d}_i \sigma^{\mu\nu} (1 + \gamma_5) T_{ij} b_j) G_{\mu\nu}, \\
 O_9 &= \frac{e}{8\pi^2} (\bar{d}b)_{V-A} (\bar{l}l)_V, \\
 O_{10} &= \frac{e}{8\pi^2} (\bar{d}b)_{V-A} (\bar{l}l)_A,
 \end{aligned} \tag{2}$$

where  $G_{\mu\nu}$  and  $F_{\mu\nu}$  are the gluon and photon field strengths, respectively;  $T_{ij}$  are the generators of the  $SU(3)$  color group;  $i$  and  $j$  denote color indices. The labels  $(V \pm A)$  stand for  $\gamma^\mu (1 \pm \gamma^5)$ .  $O_{1,2}$  are current-current operators,  $O_{3-6}$  are QCD penguin operators,  $O_{7,8}$  are magnetic penguin operators, and  $O_{9,10}$  are semileptonic electroweak penguin operators.

The most relevant contributions to  $B \rightarrow a_1 \ell^+ \ell^-$  transitions are given by the  $O_7$  and  $O_{9,10}$  short-distance (SD) contributions, as well as the tree-level four quark operators  $O_{1,2}$ , which have sizeable Wilson coefficients. The current-current operators  $O_{1,2}$  involve intermediate charm-loop LD contributions, coupled to the lepton pair via the virtual photon (see Fig. 1). This contribution has got the same form factor dependence as  $C_9$  and can therefore be absorbed into an effective Wilson coefficient  $C_9^{\text{eff}}$  [9].

Therefore, the effective Hamiltonian for  $B \rightarrow a_1 \ell^+ \ell^-$  decays, which occur via the  $b \rightarrow d \ell^+ \ell^-$  loop transition, can be written as

$$\begin{aligned}
 H_{\text{eff}} &= \frac{G_F \alpha}{2\sqrt{2}\pi} V_{tb} V_{td}^* \left[ C_9^{\text{eff}} \bar{d} \gamma_\mu (1 - \gamma_5) b \bar{l} \gamma_\mu l + C_{10} \bar{d} \gamma_\mu \right. \\
 &\quad \left. \times (1 - \gamma_5) b \bar{l} \gamma_\mu \gamma_5 l - 2C_7^{\text{eff}} \frac{m_b}{q^2} \bar{d} i \sigma_{\mu\nu} q^\nu (1 + \gamma_5) b \bar{l} \gamma_\mu l \right], \tag{3}
 \end{aligned}$$

where  $C_7^{\text{eff}} = C_7 - C_5/3 - C_6$ . The effective Wilson coefficients  $C_9^{\text{eff}}(q^2)$  are given as

$$C_9^{\text{eff}}(q^2) = C_9 + Y(q^2). \tag{4}$$

The function  $Y(q^2)$  contains the LD contributions coming from the real  $c\bar{c}$  intermediate states called charmonium resonances. Two resonances,  $J/\psi$  and  $\psi'$ , are narrow and the last four resonances,  $\psi(3370)$ ,  $\psi(4040)$ ,  $\psi(4160)$ , and  $\psi(4415)$ , are above the  $D\bar{D}$  threshold and as a consequence the width is much larger. The explicit expressions of the  $Y(q^2)$  can be found in [9] (see also [8, 10]).

To calculate the form factors of the FCNC  $B \rightarrow a_1$  transition, within the 3PSR method, we start with the following correlation functions constructed from the transition currents  $J_\mu^{V-A} = \bar{d} \gamma_\mu (1 - \gamma_5) b$  and  $J_\mu^T = \bar{d} i \sigma_{\mu\eta} q^\eta (1 + \gamma_5) b$ :

$$\begin{aligned}
 \Pi_{\mu\nu}^{V-A(T)}(p^2, p'^2, q^2) &= \int d^4x d^4y e^{-ipx} e^{ip'y} \langle 0 | \mathcal{T}[J_\nu^{a_1}(y) \\
 &\quad \times J_\mu^{V-A(T)}(0) J^{B^\dagger}(x)] | 0 \rangle, \tag{5}
 \end{aligned}$$

where  $J^B = \bar{u} \gamma_5 b$  and  $J_\nu^{a_1} = \bar{u} \gamma_\nu \gamma_5 d$  are the interpolating currents of the initial and final meson states, respectively. In the QCD sum rules approach, we can obtain the correlation functions of Eq. (5) in two languages: the hadron language, which is the physical or phenomenological side, and the quark-gluon language called the QCD or theoretical side. Equating two sides and applying the double Borel transformations with respect to the momentum of the initial and final states to suppress the contribution of the higher states and continuum, we get sum rule expressions for our form factors. To drive the phenomenological part, two complete sets of intermediate states with the same quantum numbers as the currents  $J_\nu^{a_1}$  and  $J^B$  are inserted in Eq. (5). As a result of this procedure,

$$\begin{aligned}
 \Pi_{\mu\nu}^{V-A(T)}(p, p') &= \frac{1}{p^2 - m_B^2} \frac{1}{p'^2 - m_{a_1}^2} \langle 0 | J_\nu^{a_1} | a_1 \rangle \\
 &\quad \times \langle a_1 | J_\mu^{V-A(T)} | B \rangle \langle B | J^{B^\dagger} | 0 \rangle \\
 &\quad + \text{higher states}, \tag{6}
 \end{aligned}$$

where  $p$  and  $p'$  are the momentum of the initial and final meson states, respectively. To get the transition matrix elements of the  $B \rightarrow a_1$  with various quark models, we

parameterize them in terms of the relevant form factors as

$$\begin{aligned} \langle a_1(p', \epsilon) | J_\mu^{V-A} | B(p) \rangle &= \frac{1}{m_B + m_{a_1}} \left[ 2A(q^2) i \epsilon_{\mu\lambda\alpha\beta} \epsilon^{*\lambda} \right. \\ &\quad \times p^\alpha p'^\beta + V_1(q^2) (P \cdot q) \epsilon_\mu^* \\ &\quad + V_2(q^2) (\epsilon^* \cdot p) P_\mu + V_0(q^2) \\ &\quad \left. \times (\epsilon^* \cdot p) q_\mu \right], \\ \langle a_1(p', \epsilon) | J_\mu^T | B(p) \rangle &= 2 T_1(q^2) i \epsilon_{\mu\lambda\alpha\beta} \epsilon^{*\lambda} p^\alpha p'^\beta \\ &\quad + T_2(q^2) (m_B^2 - m_{a_1}^2) \\ &\quad \times \left[ \epsilon_\mu^* - \frac{1}{q^2} (\epsilon^* \cdot q) q_\mu \right] \\ &\quad + T_3(q^2) (\epsilon^* \cdot p) \\ &\quad \times \left[ P_\mu - \frac{1}{q^2} (P \cdot p) q_\mu \right], \end{aligned} \quad (7)$$

where  $P = p + p'$  and  $q = p - p'$ . Also  $m_{a_1}$  and  $\epsilon$  are the mass and the four-polarization vector of the  $a_1$  meson. The vacuum-to-meson transition matrix elements are defined in the standard way, namely

$$\langle 0 | J^B | B \rangle = -i f_B \frac{m_B^2}{m_b}, \quad \langle 0 | J_v^{a_1} | a_1 \rangle = f_{a_1} m_{a_1} \epsilon_v. \quad (8)$$

Using Eqs. (7) and (8) in Eq. (6), and performing a summation over the polarization of the  $a_1$  meson, we obtain

$$\begin{aligned} \Pi_{\mu\nu}^{V-A} &= \frac{f_B m_B^2}{m_b} \frac{f_{a_1} m_{a_1}}{(p^2 - m_B^2)(p'^2 - m_{a_1}^2)} \\ &\quad \times \left[ \frac{2A}{m_B + m_{a_1}} (q^2) \epsilon_{\mu\nu\alpha\beta} p^\alpha p'^\beta \right. \\ &\quad - i V_1(q^2) (m_B - m_{a_1}) g_{\mu\nu} - i \frac{V_2(q^2)}{m_B + m_{a_1}} P_\mu p_\nu \\ &\quad \left. - i \frac{V_0(q^2)}{m_B + m_{a_1}} q_\mu p_\nu \right] + \text{excited states}, \\ \Pi_{\mu\nu}^T &= \frac{f_B m_B^2}{m_b} \frac{f_{a_1} m_{a_1}}{(p^2 - m_B^2)(p'^2 - m_{a_1}^2)} \\ &\quad \times \left[ 2T_1(q^2) \epsilon_{\mu\nu\alpha\beta} p^\alpha p'^\beta - i T_2(q^2) (m_B^2 - m_{a_1}^2) g_{\mu\nu} \right. \\ &\quad \left. - i T_3(q^2) P_\mu p_\nu \right] + \text{excited states}. \end{aligned} \quad (9)$$

To calculate the form factors  $A$ ,  $V_i$  ( $i = 0, 1, 2$ ), and  $T_j$  ( $j = 1, 2, 3$ ), we will choose the structures  $\epsilon_{\mu\nu\alpha\beta} p^\alpha p'^\beta$ ,  $g_{\mu\nu}$ ,  $P_\mu p_\nu$ ,  $q_\mu p_\nu$ , from  $\Pi_{\mu\nu}^{V-A}$  and  $\epsilon_{\mu\nu\alpha\beta} p^\alpha p'^\beta$ ,  $g_{\mu\nu}$ , and  $P_\mu p_\nu$  from  $\Pi_{\mu\nu}^T$ , respectively. For simplicity, the correlations are written as

$$\begin{aligned} \Pi_{\mu\nu}^{V-A}(p^2, p'^2, q^2) &= \Pi_A^{V-A} \epsilon_{\mu\nu\alpha\beta} p^\alpha p'^\beta - i \Pi_1^{V-A} g_{\mu\nu} \\ &\quad - i \Pi_2^{V-A} P_\mu p_\nu - i \Pi_0^{V-A} q_\mu p_\nu + \dots, \\ \Pi_{\mu\nu}^T(p^2, p'^2, q^2) &= \Pi_1^T \epsilon_{\mu\nu\alpha\beta} p^\alpha p'^\beta - i \Pi_2^T g_{\mu\nu} \\ &\quad - i \Pi_3^T P_\mu p_\nu + \dots. \end{aligned} \quad (10)$$

Now, we consider the theoretical part of the sum rules. To this aim, each  $\Pi_k^{V-A(T)}$  function is defined in terms of the perturbative and nonperturbative parts as

$$\Pi^{V-A(T)}(p^2, p'^2, q^2) = \Pi_{\text{per}}^{V-A(T)}(p^2, p'^2, q^2) + \Pi_{\text{nonper}}^{V-A(T)}(p^2, p'^2, q^2). \quad (11)$$

For the perturbative part, the bare-loop diagrams are considered. With the help of the double dispersion representation, the bare-loop contribution is written as

$$\begin{aligned} \Pi_{\text{per}}^{V-A(T)} &= -\frac{1}{(2\pi)^2} \int ds' \int ds \\ &\quad \times \frac{\rho^{V-A(T)}(s, s', q^2)}{(s - p^2)(s' - p'^2)} + \text{subtraction terms}, \end{aligned}$$

where  $\rho$  is the spectral density. The spectral density is obtained from the usual Feynman integral for the bare loop by replacing  $\frac{1}{p^2 - m^2} \rightarrow -2\pi i \delta(p^2 - m^2)$ . After standard calculations for the spectral densities  $\rho_k^{V-A(T)}$ , where  $k$  is related to each structure in Eq. (10), we have

$$\begin{aligned} \rho_A^{V-A} &= 3s' \Lambda^{-3} (u - 2\Delta) m_b, \\ \rho_0^{V-A} &= -\frac{3}{2} s' \Lambda^{-5} \left( 12u\Delta s' - 4ss'^2 - 2u^2s' - 12s'\Delta^2 \right. \\ &\quad \left. - 2sus' - 6u\Delta^2 - u^3 + 6u^2\Delta \right) m_b, \\ \rho_1^{V-A} &= -\frac{3}{2} s' \Lambda^{-3} \left( 2ss' - 2\Delta^2 + 2\Delta u - u^2 \right) m_b, \\ \rho_2^{V-A} &= -\frac{3}{2} s' \Lambda^{-5} \left( 12u\Delta s' - 4ss'^2 - 2u^2s' - 12s'\Delta^2 \right. \\ &\quad \left. + 2sus' + 6u\Delta^2 + u^3 - 6u^2\Delta \right) m_b, \\ \rho_1^T &= -3s' \Lambda^{-3} (u - 2\Delta) m_b^2, \\ \rho_2^T &= \frac{3}{2} s' \Lambda^{-3} \left( 2s^2s' - 2s\Delta^2 + 2s\Delta u - su^2 \right. \\ &\quad \left. - 4ss'\Delta + sus' + u\Delta^2 \right), \\ \rho_3^T &= \frac{3}{2} s' \Lambda^{-5} \left( 4s^2s'^2 + 2us^2s' + 6sus'^2 - 8ss'^2\Delta \right. \\ &\quad + 8\Delta uss' - 4ss'\Delta^2 - 7su^2s' + su^3 \\ &\quad - 6su^2\Delta + 6su\Delta^2 + 6u\Delta^2s' - 4u^2\Delta s' \\ &\quad \left. + 4\Delta u^3 - 5u^2\Delta^2 \right), \end{aligned} \quad (12)$$

where  $u = s + s' - q^2$ ,  $\Lambda = \sqrt{u^2 - 4ss'}$ , and  $\Delta = s - m_b^2$ .

Now the nonperturbative part contributions to the correlation functions are discussed [Eq. (11)]. In QCD, the three-point correlation function can be evaluated by the operator

product expansion (OPE) in the deep Euclidean region. Up to dimension 6, the operators are determined by the contribution of the bare-loop, and power corrections coming from dimension-3  $\langle \bar{\psi}\psi \rangle$ , dimension-4  $\langle G^2 \rangle$ , dimension-5  $m_0^2 \langle \bar{\psi}\psi \rangle$ , and dimension-6  $\langle \bar{\psi}\psi \rangle^2$  operators [5]. The bare-loop diagrams, the perturbative part of the correlation functions, have been discussed before. For the nonperturbative part contributions, our calculations show that the contributions coming from  $\langle G^2 \rangle$  and  $\langle \bar{\psi}\psi \rangle^2$  are very small in comparison with the contributions of dimension 3 and 5, and that the former contributions can easily be ignored. We introduce the nonperturbative part contributions as

$$\Pi_{\text{nonper}}^{V-A}(T) = \langle u\bar{u} \rangle C^{V-A}(T), \tag{13}$$

where  $\langle u\bar{u} \rangle = -(0.240 \pm 0.010)^3 \text{ GeV}^3$  [11]. After some straightforward calculations, the explicit expressions for  $C_k^{V-A}(T)$  are given by

$$\begin{aligned} C_A^{V-A} &= \frac{1}{rr'} - m_0^2 \left[ \frac{1}{3r^2r'} + \frac{m_b^2 - q^2}{3r^2r'^2} + \frac{m_b^2}{2r^3r'} \right], \\ C_0^{V-A} &= \frac{1}{rr'} - m_0^2 \left[ \frac{1}{r^2r'} + \frac{m_b^2 - q^2}{3r^2r'^2} + \frac{m_b^2}{2r^3r'} \right], \\ C_1^{V-A} &= \frac{(m_b^2 - q^2)}{2rr'} - m_0^2 \left[ -\frac{1}{6rr'} + \frac{m_b^2 - q^2}{6r'^2} \right. \\ &\quad \left. + \frac{3m_b^2 - 4q^2}{12r^2r'} + \frac{(m_b^2 - q^2)^2}{6r^2r'^2} + \frac{m_b^4 - m_b^2q^2}{4r^3r'} \right], \\ C_2^{V-A} &= -\frac{1}{rr'} - m_0^2 \left[ \frac{1}{3r^2r'} - \frac{m_b^2 - q^2}{3r^2r'^2} - \frac{m_b^2}{2r^3r'} \right], \\ C_1^T &= -\frac{m_b}{rr'} - m_0^2 \left[ -\frac{m_b}{2r^2r'} - \frac{m_b(m_b^2 - q^2)}{3r^2r'^2} - \frac{m_b^3}{2r^3r'} \right], \\ C_2^T &= \frac{(-m_b^3 + m_bq^2)}{2rr'} - m_0^2 \left[ -\frac{m_b}{4rr'} - \frac{m_b(m_b^2 - q^2)}{6r'^2} \right. \\ &\quad \left. - \frac{m_b(4m_b^2 - 5q^2)}{12r^2r'} - \frac{m_b(m_b^2 - q^2)^2}{6r^2r'^2} \right. \\ &\quad \left. - \frac{m_b^5 - m_b^3q^2}{4r^3r'} \right], \\ C_3^T &= \frac{m_b}{2rr'} - m_0^2 \left[ \frac{2m_b}{3r^2r'} + \frac{m_b(m_b^2 - q^2)}{8r^2r'^2} + \frac{m_b^3}{4r^3r'} \right], \tag{14} \end{aligned}$$

where  $r = p^2 - m_b^2$ ,  $r' = p'^2$ , and  $m_0^2 = (0.8 \pm 0.2) \text{ GeV}^2$  [11].

The next step is to apply the Borel transformations as

$$B_{p^2}(M^2) \left( \frac{1}{p^2 - m^2} \right)^n = \frac{(-1)^n e^{-m^2/M^2}}{\Gamma(n) (M^2)^n}, \tag{15}$$

with respect to the  $p^2(p^2 \rightarrow M_1^2)$  and  $p'^2(p'^2 \rightarrow M_2^2)$  on the phenomenological as well as the perturbative and nonperturbative parts of the correlation functions and equate these

two representations of the correlations. The following sum rules for the form factors are derived:

$$\begin{aligned} A'(V'_i)(q^2) &= -\frac{m_b}{f_B m_B^2 f_{a_1} m_{a_1}} e^{m_b^2/M_1^2} e^{m_{a_1}^2/M_2^2} \\ &\quad \times \left\{ -\frac{1}{4\pi^2} \int_0^{s'_0} ds' \int_{s_L}^{s_0} ds \rho_{A(i)}^{V-A} e^{-s/M_1^2} e^{-s'/M_2^2} \right. \\ &\quad \left. + \langle u\bar{u} \rangle \times B_{p^2}(M_1^2) B_{p^2}(M_2^2) C_{A(i)}^{V-A} \right\}, \\ T'_j(q^2) &= -\frac{m_b}{f_B m_B^2 f_{a_1} m_{a_1}} e^{m_b^2/M_1^2} e^{m_{a_1}^2/M_2^2} \\ &\quad \times \left\{ -\frac{1}{4\pi^2} \int_0^{s'_0} ds' \int_{s_L}^{s_0} ds \rho_j^T e^{-s/M_1^2} e^{-s'/M_2^2} \right. \\ &\quad \left. + \langle u\bar{u} \rangle \times B_{p^2}(M_1^2) B_{p^2}(M_2^2) C_j^T \right\}, \tag{16} \end{aligned}$$

where

$$\begin{aligned} A'(q^2) &= \frac{2A(q^2)}{m_B + m_{a_1}}, & V'_0(q^2) &= \frac{V_0(q^2)}{m_B + m_{a_1}}, \\ V'_1(q^2) &= V_1(q^2)(m_B - m_{a_1}), & V'_2(q^2) &= \frac{V_2(q^2)}{m_B + m_{a_1}}, \\ T'_1(q^2) &= 2T_1(q^2), & T'_2(q^2) &= T_2(q^2)(m_B^2 - m_{a_1}^2), \\ T'_3(q^2) &= T_3(q^2). \end{aligned}$$

$s_0$  and  $s'_0$  are the continuum thresholds in the  $B$  and  $a_1$  meson channels, respectively.  $s_L$ , the lower limit of the integration over  $s$ , is  $m_b^2 + \frac{m_b^2}{m_b^2 - q^2} s'$ .

### 3 Numerical analysis

In this section, we present our numerical analysis of the form factors  $A$ ,  $V_i$ , and  $T_j$ . We choose the values of the quark, lepton, and meson masses and also the leptonic decay constants thus:  $m_b = 4.8 \text{ GeV}$  [12],  $m_\mu = 0.105 \text{ GeV}$ ,  $m_\tau = 1.776 \text{ GeV}$ ,  $m_{a_1} = 1.260 \text{ GeV}$ ,  $m_B = 5.280 \text{ GeV}$  [13],  $f_{a_1} = (238 \pm 10) \text{ MeV}$  [14]. For the value of the  $f_B$ , we shall use  $f_B = 140 \text{ MeV}$ . This value of  $f_B$  corresponds to the case where  $\mathcal{O}(\alpha_s)$  corrections are not taken into account (see [15, 16]).

The sum rules for the form factors contain also four auxiliary parameters: the Borel mass squares  $M_1^2$  and  $M_2^2$  and the continuum thresholds  $s_0$  and  $s'_0$ . These are not physical quantities, so the form factors as physical quantities should be independent of them. The continuum thresholds of  $B$  and  $a_1$  mesons,  $s_0$  and  $s'_0$ , respectively, are not completely arbitrary; they are correlated with the energy of the first excited state with the same quantum numbers as the considered interpolating currents. The values of the continuum thresholds calculated from the two-point QCD sum rules are taken to be  $s_0 = (35 \pm 2) \text{ GeV}^2$  [17] and  $s'_0 = (2.55 \pm 0.15) \text{ GeV}^2$  [14]. We search for the intervals of the Borel mass parameters so that our results are almost insensitive to their variations. One

**Table 1** The values of the  $b_r$  related to  $F^{(1)}(q^2)$

Parameter	$A^{(1)}$	$V_0^{(1)}$	$V_1^{(1)}$	$V_2^{(1)}$	$T_1^{(1)}$	$T_2^{(1)}$	$T_3^{(1)}$
$b_0$	0.44	0.35	0.28	-0.30	-0.33	-0.21	0.33
$b_1$	0.80	1.77	2.80	-1.79	-0.60	-2.14	1.42
$b_2$	3.89	0.09	15.52	0.94	-2.90	-11.34	-0.04

**Table 2** The values of the  $f(0)$ ,  $\alpha$ , and  $\beta$  connected to  $F^{(2)}(q^2)$

Parameter	$A^{(2)}$	$V_0^{(2)}$	$V_1^{(2)}$	$V_2^{(2)}$	$T_1^{(2)}$	$T_2^{(2)}$	$T_3^{(2)}$
$f(0)$	0.51	0.46	0.52	-0.41	-0.37	-0.37	0.41
$\alpha$	0.58	0.37	-0.52	0.34	0.58	-0.50	0.44
$\beta$	-0.39	-0.04	0.38	0.14	-0.40	0.48	-0.10

**Table 3** Transition form factors of the  $B \rightarrow a_1 \ell \nu$  at  $q^2 = 0$  in various models. The results of other methods have been rescaled according to the form factor definition in Eq. (7)

Model	$A(0)$	$V_0(0)$	$V_1(0)$	$V_2(0)$
LFQM [2]	0.67	0.34	0.37	-0.29
CQM [3]	0.23	3.11	1.32	-0.55
LCSR [4]	$0.48 \pm 0.09$	$0.77 \pm 0.13$	$0.60 \pm 0.11$	$-0.42 \pm 0.08$
SR [5]	$0.55 \pm 0.08$	$0.49 \pm 0.11$	$0.56 \pm 0.07$	$-0.43 \pm 0.04$
This work	$0.51 \pm 0.11$	$0.46 \pm 0.10$	$0.52 \pm 0.11$	$-0.41 \pm 0.09$

more condition for the intervals of these parameters is the fact that the aforementioned intervals must suppress the higher states and continuum, and contributions of the highest-order operators. In other words, the sum rules for the form factors must converge (for more details, see [18]). As a result, we get  $8 \text{ GeV}^2 \leq M_1^2 \leq 15 \text{ GeV}^2$  and  $2.5 \text{ GeV}^2 \leq M_2^2 \leq 4 \text{ GeV}^2$ .

Equation (16) shows the  $q^2$  dependence of the form factors in the region where the sum rule is valid. To extend these results to the full region, we look for a parametrization of the form factors in such a way that, in the validity region of the 3PSR, this parametrization coincides with the sum rules prediction. We use the two following sufficient parametrizations of the form factors with respect to  $q^2$ :

$$F^{(1)}(q^2) = \frac{1}{1 - \left(\frac{q^2}{m_B^2}\right)} \sum_{r=0}^2 b_r \left[ z^r + (-1)^r \frac{r}{3} z^4 \right], \quad (17)$$

where  $z = \frac{\sqrt{t_+ - q^2} - \sqrt{t_+ - t_0}}{\sqrt{t_+ - q^2} + \sqrt{t_+ - t_0}}$ ,  $t_+ = (m_B + m_{a_1})^2$ , and  $t_0 = (m_B + m_{a_1})(\sqrt{m_B} - \sqrt{m_{a_1}})^2$  [19], and also

$$F^{(2)}(q^2) = \frac{f(0)}{1 - \alpha \left(\frac{q^2}{m_B^2}\right) + \beta \left(\frac{q^2}{m_B^2}\right)^2}. \quad (18)$$

We evaluated the values of the parameters  $b_r$  ( $r = 1, \dots, 3$ ) of the first and  $f(0)$ ,  $\alpha$ ,  $\beta$  of the second fit function for each transition form factor of the  $B \rightarrow a_1$  decay, taking  $M_1^2 = 10 \text{ GeV}^2$  and  $M_2^2 = 3 \text{ GeV}^2$ . Tables 1 and 2 show the values of the  $b_r$  and  $f(0)$ , and  $\alpha$ ,  $\beta$  for the form factors.

So far, several authors have calculated the form factors of the  $B \rightarrow a_1 \ell \nu$  decay via the different approaches. For a comparison, the form factor predictions of the other approaches at  $q^2 = 0$  are shown in Table 3. The results of other methods have been rescaled according to the form factor definition in Eq. (7). It is useful to present the relations between our form factors ( $A, V_i$ ) in Eq. (7) to those used in [2–5]. The relations read

$$A = \frac{(m_B + m_{a_1})}{(m_B - m_{a_1})} A^{[2]} = -A^{[3]}, \quad V_0 = -\frac{(m_B + m_{a_1})}{2m_{a_1}} V_0^{[2,3]},$$

$$V_1 = V_1^{[2]} = -\frac{(m_B + m_{a_1})}{(m_B - m_{a_1})} V_1^{[3]}, \quad V_2 = -\frac{(m_B + m_{a_1})}{(m_B - m_{a_1})} V_2^{[2]} = V_2^{[3]}.$$

Also, the relation between our form factors and those used in [4] and [5] are obtained from the above equations by replacing  $A^{[3]} \rightarrow -A^{[4]}$ ,  $V_i^{[3]} \rightarrow -V_i^{[4]}$ , and  $A^{[3]} \rightarrow \kappa A^{[5]}$ ,  $V_i^{[3]} \rightarrow \kappa V_i^{[5]}$ , respectively, where  $\kappa = \frac{\sqrt{2} m_{a_1}}{g_{a_1} f_{a_1}}$ .

The errors in Table 3 are estimated by the variation of the Borel parameters  $M_1^2$  and  $M_2^2$ , the variation of the continuum thresholds  $s_0$  and  $s'_0$ , and the variation of the  $b$  quark mass and leptonic decay constants  $f_B$  and  $f_{a_1}$ . The main uncertainty comes from the thresholds and the decay constants, which is about  $\sim 25\%$  of the central value, while the other uncertainties are small, constituting a few percent.

The dependence of the form factors,  $A^{(1)}, V_i^{(1)}, T_j^{(1)}(q^2)$ , and  $A^{(2)}, V_i^{(2)}, T_j^{(2)}$  on  $q^2$  extracted from the fit functions, Eqs. (17) and (18), are given in Figs. 2 and 3, respectively.

In the standard model, the rare semileptonic  $B \rightarrow a_1 \ell^+ \ell^-$  and  $B \rightarrow \rho \ell^+ \ell^-$  decays are described via loop transitions,  $b \rightarrow d \ell^+ \ell^-$  at quark level. The two mesons  $a_1$  and  $\rho$  have the same quark content but different masses and parities,

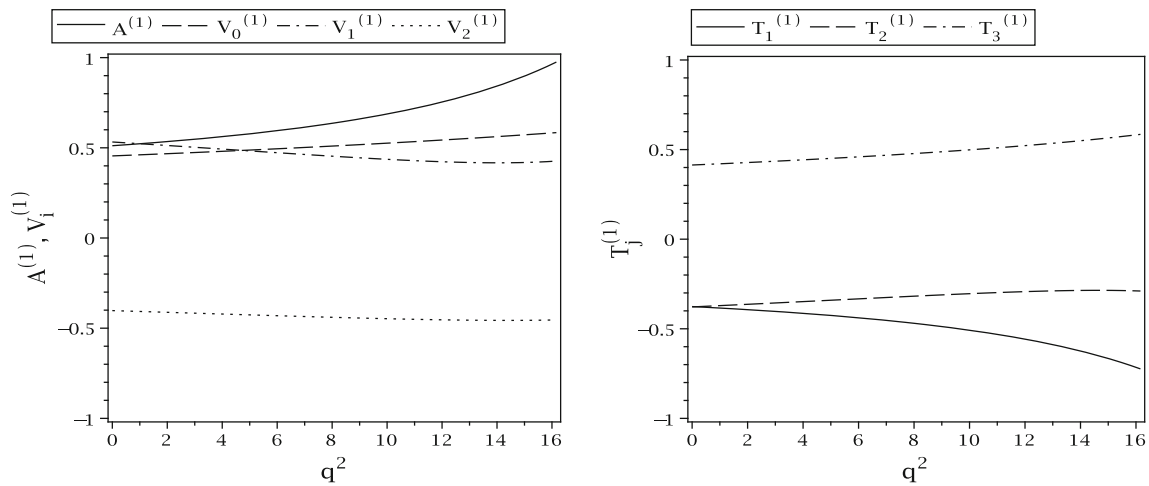


**Fig. 2** The form factors  $A^{(1)}$ ,  $V_i^{(1)}$  and  $T_j^{(1)}$  on  $q^2$

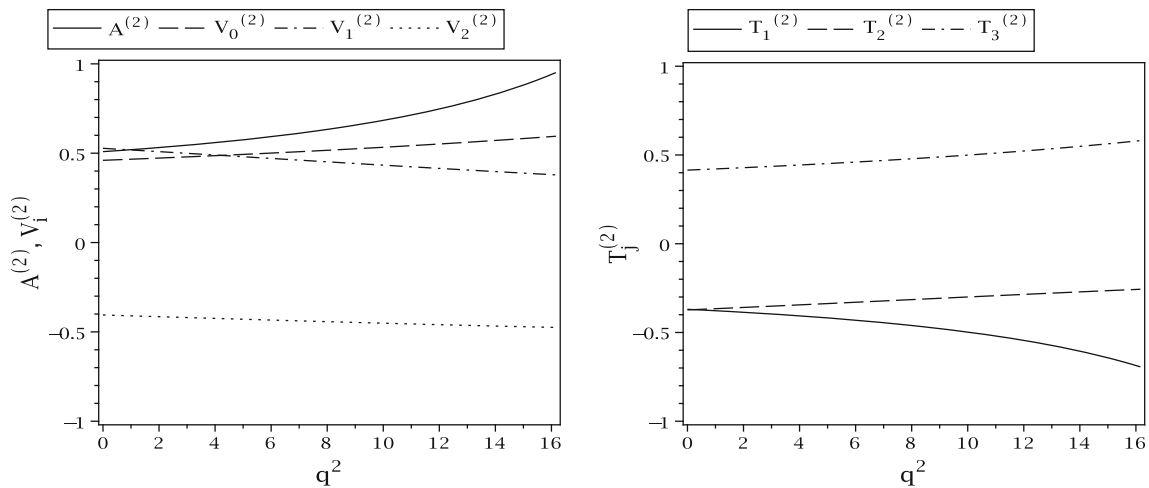


**Fig. 3** The form factors  $A^{(2)}$ ,  $V_i^{(2)}$ , and  $T_j^{(2)}$  on  $q^2$

**Table 4** The form factor values of the  $B \rightarrow \rho \ell^+ \ell^-$  at  $q^2 = 0$

Mode	$V(0)$	$A_0(0)$	$A_1(0)$	$A_2(0)$	$T_1(0)$	$T_2(0)$	$T_3(0)$
This work	$0.30 \pm 0.09$	$0.29 \pm 0.08$	$0.24 \pm 0.06$	$0.20 \pm 0.07$	$0.26 \pm 0.07$	$0.26 \pm 0.07$	$0.16 \pm 0.05$
LCSR [20]	0.32	0.30	0.24	0.22	0.27	0.27	0.18

i.e.,  $\rho$  is a vector ( $1^-$ ) and  $a_1$  is an axial vector ( $1^+$ ). We have calculated the form-factor values of the  $B \rightarrow \rho \ell^+ \ell^-$  at  $q^2 = 0$  in the SR model shown in Table 4. Also, this table contains the results estimated for these form factors in the frame work of the LCSR. The values predicted by us and the LCSR model are very close to each other in many cases. If  $a_1$  behaves as the scalar partner of the  $\rho$  meson, it is expected that the  $A(0)$  for the  $B \rightarrow a_1$  decays is similar to the  $V(0)$  for the  $B \rightarrow \rho$  transitions, for example. The values obtained for  $A(0)$  via two the SR and LCSR models in Table 3 are larger than those for  $V(0)$  in Table 4. It appears to us that

the transition form factors of the  $B \rightarrow a_1$  decays are quite different from those for  $B \rightarrow \rho$ .

Now, we would like to evaluate the branching ratio values for the  $B \rightarrow a_1 \ell^+ \ell^-$  decays. The expressions of the differential decay widths  $d\Gamma/dq^2$  for the  $B \rightarrow a_1 \nu \bar{\nu}$  and  $B \rightarrow a_1 \ell^+ \ell^-$  decays can be found in [21,22]. These expressions contain the Wilson coefficients  $C_7^{\text{eff}}$ ,  $C_9^{\text{eff}}$ ,  $C_{10}$ , and also the CKM matrix elements  $V_{tb}$  and  $V_{td}$ . Considering  $C_7^{\text{eff}} = -0.313$ ,  $C_{10} = -4.669$ ,  $|V_{tb}V_{td}^*| = 0.008$  [8], and the form factors related to the fit functions, Eqs. (17) and (18), and after numerical analysis, the branching ratios for

**Table 5** The branching ratios of the semileptonic  $B \rightarrow a_1 \ell^+ \ell^-$  decays, considering two groups of the form factors. 1 and 2 stand for the form factors,  $F^{(1)}$  and  $F^{(2)}$ , respectively

Mode	Form factors	Value
$\text{Br}(B \rightarrow a_1 \nu \bar{\nu}) \times 10^8$	1	$7.41 \pm 2.44$
	2	$7.78 \pm 2.32$
$\text{Br}(B \rightarrow a_1 e^+ e^-) \times 10^8$	1	$2.75 \pm 0.58$
	2	$2.90 \pm 0.95$
$\text{Br}(B \rightarrow a_1 \mu^+ \mu^-) \times 10^8$	1	$2.54 \pm 0.47$
	2	$2.70 \pm 0.89$
$\text{Br}(B \rightarrow a_1 \tau^+ \tau^-) \times 10^9$	1	$0.37 \pm 0.09$
	2	$0.33 \pm 0.10$

the  $B \rightarrow a_1 \ell^+ \ell^- / \nu \bar{\nu}$  are obtained as presented in Table 5. In this table, we show only the values obtained considering the SD effects contributing to the Wilson coefficient  $C_9^{\text{eff}}$  in Eq. (4) for the charged lepton case.

In this part, we would like to present the branching ratio values including LD effects via  $C_9^{\text{eff}}$ . Due to the fact that in our calculations  $q^2 < m_{\psi(4040)}^2$ , we introduce some cuts around the narrow resonances of the  $J/\psi$  and  $\psi'$ , and we study the following three regions for the muon:

$$\begin{aligned}
 \text{I} : & 2m_\mu \leq \sqrt{q^2} \leq M_{J/\psi} - 0.20, \\
 \text{II} : & M_{J/\psi} + 0.04 \leq \sqrt{q^2} \leq M_{\psi'} - 0.10, \\
 \text{III} : & M_{\psi'} + 0.02 \leq \sqrt{q^2} \leq m_B - m_{a_1},
 \end{aligned} \tag{19}$$

and the following two for the tau:

$$\begin{aligned}
 \text{I} : & 2m_\tau \leq \sqrt{q^2} \leq M_{\psi'} - 0.02, \\
 \text{II} : & M_{\psi'} + 0.02 \leq \sqrt{q^2} \leq m_B - m_{a_1}.
 \end{aligned} \tag{20}$$

In Table 6, we present the branching ratios for muon and tau obtained using the regions shown in Eqs. (19) and (20), respectively. In our calculations, two groups of form factors are considered. Here, we should also stress that the results obtained for the electron are very close to the results of the muon, and for this reason we only present the branching ratios for the muon in our table.

Considering the form factors,  $F^{(1)}$  and  $F^{(2)}$ , the dependency of the differential branching ratios on  $q^2$  with and without LD effects for charged lepton case is shown in Fig. 4. In this figure, the solid and dash-dotted lines show the results without and with the LD effects, respectively, using

the form factors,  $F^{(1)}$ . Also, the circles and stars are the same as those lines but considering  $F^{(2)}$  this time.

In Ref. [9], the interference pattern of the charm-resonances  $J/\psi$  (3370, 4040, 4160, 4415) with the electroweak penguin operator  $O_9$  in the branching fraction of  $B^+ \rightarrow K^+ \mu^+ \mu^-$  has been investigated (in this case  $q^2 \simeq 22 \text{ GeV}^2$ ). For this purpose, the charm vacuum polarization via a standard dispersion relation from BESII-data on  $e^+ e^- \rightarrow$  hadrons is extracted. In the factorization approximation the vacuum polarization describes the interference fully non-perturbatively. The observed interference pattern by the LHCb collaboration is opposite in sign and significantly enhanced as compared to factorization approximation. A change of the factorization approximation result by a factor of  $-2.5$ , which corresponds to a 350 %-correction, results in a reasonable agreement with the data.

Finally, we want to calculate the longitudinal lepton polarization asymmetry and the forward-backward asymmetry for the decays considered. The expressions of the longitudinal lepton polarization asymmetry and the forward-backward asymmetry,  $P_L$  and  $A_{FB}$ , are given in [21, 22].

The dependence of the longitudinal lepton polarization and the forward-backward asymmetries for the  $B \rightarrow a_1 \ell^+ \ell^-$  decays on the transferred momentum square  $q^2$  with and without LD effects are plotted in Figs. 5 and 6, respectively.

The measurements of these quantities in the FCNC transitions are difficult. Among the large set of inclusive and exclusive FCNC modes, considerable attention has been put into  $B \rightarrow K^* \mu^+ \mu^-$  such as: measurement of the differential branching fraction and forward-backward asymmetry for  $B \rightarrow K^* \ell^+ \ell^-$  [23], and measurements of the angular distributions in the decays  $B \rightarrow K^* \mu^+ \mu^-$  [24], and differential branching fraction and angular analysis of the decay  $B \rightarrow K^* \mu^+ \mu^-$  [25]; and also the angular distributions in the decay  $B \rightarrow K^* \ell^+ \ell^-$  [26, 27]. In Ref. [27], measurements of the BABAR are presented for the FCNC decays,  $B \rightarrow K^* \ell^+ \ell^-$ , including branching fractions, isospin asymmetries, direct CP violation, and lepton flavor universality for dilepton masses below and above the  $J/\psi$  resonance. Furthermore, BABAR results from an angular analysis in  $B \rightarrow K^* \ell^+ \ell^-$  are reported in which both the  $K^*$  longitudinal polarization and the lepton forward-backward asymmetry are measured for dilepton masses below and above the  $J/\psi$  resonance.

**Table 6** The branching ratios of the semileptonic  $B \rightarrow a_1 \ell^+ \ell^-$  decays including LD effects in three regions. 1 and 2 stand for the form factors,  $F^{(1)}$  and  $F^{(2)}$ , respectively

Mode	form factors	I	II	III	I + II + III
$\text{Br}(B \rightarrow a_1 \mu^+ \mu^-) \times 10^8$	1	$2.07 \pm 0.68$	$0.27 \pm 0.09$	$0.08 \pm 0.03$	$2.42 \pm 0.80$
	2	$2.30 \pm 0.76$	$0.26 \pm 0.09$	$0.07 \pm 0.03$	$2.63 \pm 0.88$
$\text{Br}(B \rightarrow a_1 \tau^+ \tau^-) \times 10^9$	1	Undefined	$0.11 \pm 0.04$	$0.15 \pm 0.05$	$0.26 \pm 0.09$
	2	Undefined	$0.10 \pm 0.03$	$0.13 \pm 0.04$	$0.23 \pm 0.07$

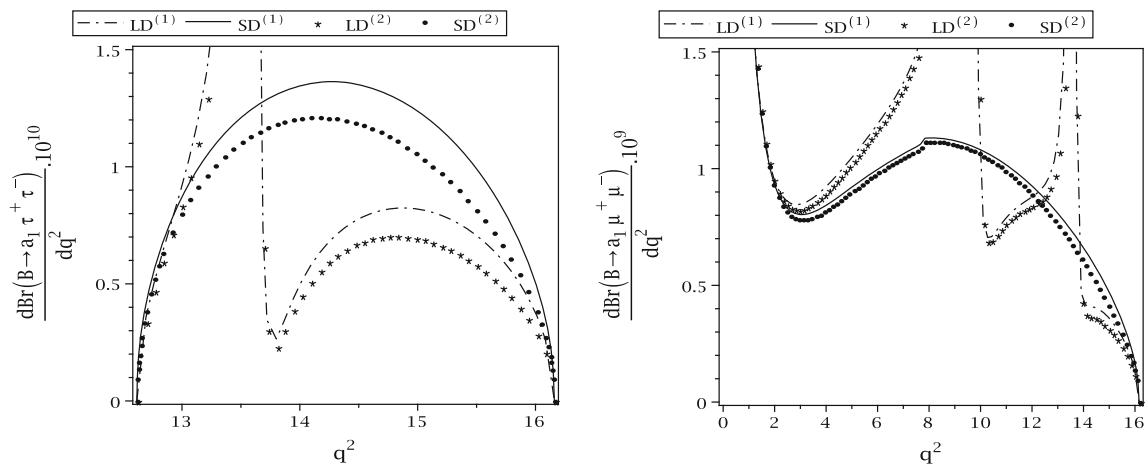


Fig. 4 The differential branching ratios of the semileptonic  $B \rightarrow a_1$  decays on  $q^2$  with and without LD effects

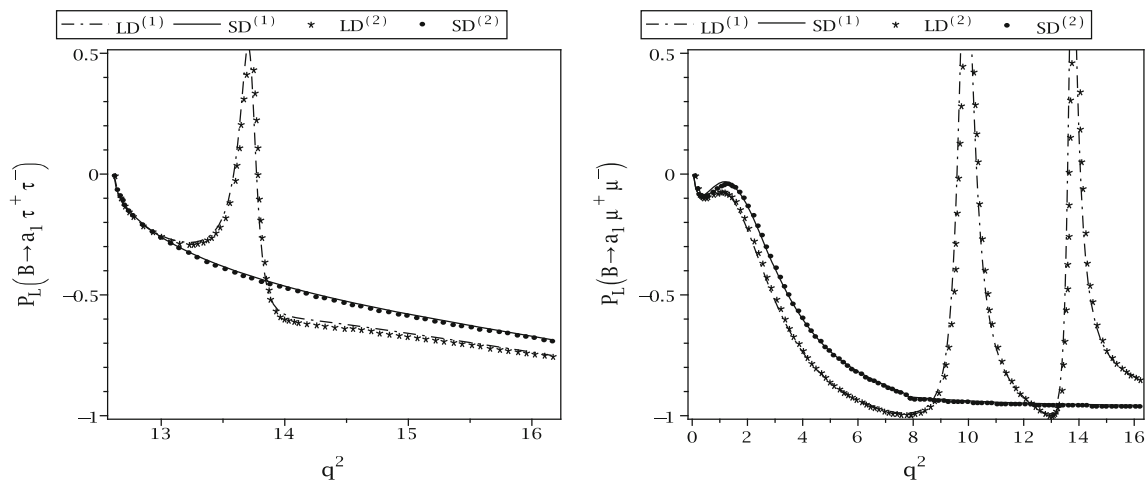


Fig. 5 The dependence of the longitudinal lepton polarization asymmetry on  $q^2$  with and without the LD effects

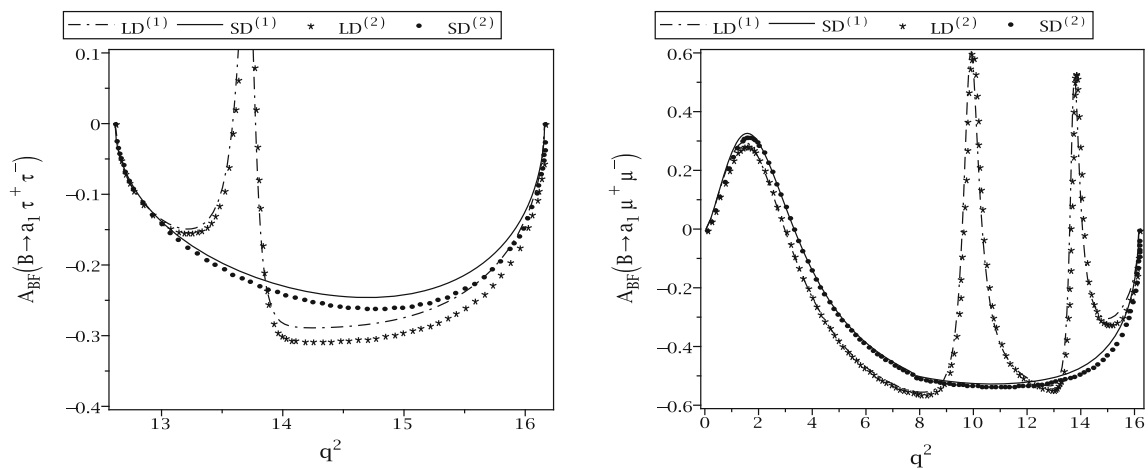


Fig. 6 The dependence of the forward–backward asymmetry on  $q^2$  with and without the LD effects



In summary, the transition form factors of the semileptonic  $B \rightarrow a_1 \ell^+ \ell^- / \nu \bar{\nu}$  decays were investigated in the 3PSR approach. Considering both the SD and the LD effects contributing to the Wilson coefficient  $C_9^{\text{eff}}$  for charged lepton case, we estimated the branching ratio values for these decays. Also, for a better analysis, the dependence of the longitudinal lepton polarization and forward–backward asymmetries of these decays on  $q^2$  are plotted.

**Acknowledgments** I would like to thank M. Haghghat for useful discussions. Partial support of the Isfahan University of Technology research council is appreciated.

**Open Access** This article is distributed under the terms of the Creative Commons Attribution 4.0 International License (<http://creativecommons.org/licenses/by/4.0/>), which permits unrestricted use, distribution, and reproduction in any medium, provided you give appropriate credit to the original author(s) and the source, provide a link to the Creative Commons license, and indicate if changes were made. Funded by SCOAP<sup>3</sup>.

## References

1. A. Deandrea, A.D. Polosa, Phys. Rev. D **64**, 074012 (2001)
2. H.Y. Cheng, C.K. Chua, C.W. Hwang, Phys. Rev. D **69**, 074025 (2004)
3. A. Deandrea, R. Gatto, G. Nardulli, A.D. Polosa, Phys. Rev. D **59**, 074012 (1999)
4. K.C. Yang, Phys. Rev. D **78**, 034018 (2008)
5. T.M. Aliev, M. Savci, Phys. Lett. B **456**, 256 (1999)
6. A. Khodjamirian, T. Mannel, A.A. Pivovarov, Y.M. Wang, JHEP **1009**, 089 (2010)
7. J. Charles et al., CKMfitter Group, Eur. Phys. J. C **41**, 1 (2005)
8. A. Faessler, Th Gutsche, M.A. Ivanov, J.G. Korner, V.E. Lyubovitskij, Eur. Phys. J. C **4**, 18 (2002)
9. J. Lyon, R. Zwicky, [arXiv:1406.0566](https://arxiv.org/abs/1406.0566) [hep-ph]
10. A.J. Buras, M. Muenz, Phys. Rev. D **52**, 186 (1995)
11. P. Colangelo, A. Khodjamirian, in *At the Frontier of Particle Physics/Handbook of QCD*, ed. by M. Shifman (World Scientific, Singapore, 2001), vol. III, p. 1495
12. K.C. Bowler et al., UKQCD Collaboration, Phys. Rev. D **52**, 5067 (1995)
13. J. Beringer et al., Particle Data Group, Phys. Rev. D **86**, 010001 (2012)
14. K.C. Yang, Nucl. Phys. B **776**, 187 (2007)
15. T.M. Aliev, V.L. Eletsky, Sov. J. Nucl. Phys. **38**, 936 (1983)
16. V.M. Belyaev, V.M. Braun, A. Khodjamirian, R. Rückl, Phys. Rev. D **51**, 6177 (1995)
17. M.A. Shifman, A.I. Vainshtein, V.I. Zakharov, Nucl. Phys. B **147**, 385 (1979)
18. P. Colangelo, A. Khodjamirian, [arXiv:0010175](https://arxiv.org/abs/0010175) [hep-ph]
19. C. Bourrely, I. Caprini, L. Lellouch, Phys. Rev. D **79**, 013008 (2009)
20. P. Ball, R. Zwicky, Phys. Rev. D **71**, 014029 (2005)
21. C.Q. Geng, C.C. Liu, J. Phys. G **29**, 1103 (2003)
22. R. Khosravi, F. Falahati, Phys. Rev. D **88**, 056002 (2013)
23. J.T. Wei et al., Belle Collaboration, Phys. Rev. Lett. **103**, 171801 (2009)
24. T. Aaltonen et al., CDF Collaboration, Phys. Rev. Lett. **108**, 081807 (2012)
25. R. Aaij et al., LHCb Collaboration, JHEP. **1308**, 131 (2013)
26. B. Aubert et al., BaBar Collaboration, Phys. Rev. D **79**, 031102 (2009)
27. G. Eigen (FPCP08 conference), [arXiv:0807.4076](https://arxiv.org/abs/0807.4076) [hep-ex]